



1 Deposition of ionic species and black carbon to the Arctic 2 snow pack: Combining snow pit observations with modeling

3 Hans-Werner Jacobi¹, Friedrich Obleitner², Sophie Da Costa¹, Patrick Ginot^{1,3}, Kostas
4 Eleftheriadis⁴, Wenche Aas⁵, and Marco Zanatta^{1,6}

5 ¹Institute for Geosciences and Environmental Research (IGE), Univ. Grenoble Alpes / CNRS / Grenoble INP /
6 IRD, Grenoble, France

7 ²Institute of Atmospheric and Cryospheric Sciences, University of Innsbruck, Austria

8 ³Observatoire des Sciences de l'Univers de Grenoble (OSUG), Univ. Grenoble Alpes / IRD / CNRS / Irstea /
9 Météo France, Grenoble, France

10 ⁴ERL, Institute of Nuclear & Radiological Sciences & Technology, Energy and Safety, NCSR Demokritos,
11 Athens, Greece

12 ⁵Norwegian Institute for Air Research, Kjeller, Norway

13 ⁶Now at: Alfred Wegener Institute (AWI), Helmholtz Centre for Polar and Marine Research, Bremerhaven,
14 Germany

15 *Correspondence to:* Hans-Werner.Jacobi@univ-grenoble-alpes.fr

16 **Abstract.** Although aerosols in the Arctic have multiple and complex impacts on the regional climate, their
17 removal due to deposition is still not well quantified. We combined meteorological, aerosol, precipitation, and
18 snow pack observations with simulations to derive information about the deposition of sea salt components and
19 black carbon (BC) from November 2011 to April 2012 to the Arctic snow pack at two locations close to Ny-
20 Ålesund, Svalbard. The dominating role of sea salt and the contribution of dust for the composition of
21 atmospheric aerosols were reflected in the seasonal composition of the snow pack. The strong alignment of the
22 concentrations of the major sea salt components in the aerosols, the precipitation, and the snow pack is linked to
23 the importance of wet deposition for the transfer from the atmosphere to the snow pack. This agreement was less
24 strong for monthly snow budgets and deposition indicating important relocation of the impurities inside the snow
25 pack after deposition. Wet deposition was less important for the transfer of nitrate, non sea salt-sulfate, and BC
26 to the snow during the winter period. The average BC concentration in the snow pack remains small with a
27 limited impact on snow albedo and melting. Nevertheless, the observations also indicate an important
28 redistribution of BC in the snowpack leading to layers with enhanced concentrations. The complex behavior of
29 bromide due to modifications during the sea salt aerosol formation and remobilization in the atmosphere and in
30 the snow were not resolved due to the lack of measurements in aerosols and precipitation.

31 1 Introduction

32 Aerosols and specifically black carbon (BC) play an important role in the regional climate of the Arctic
33 (Shindell, 2007; Quinn et al., 2007) since they modify the radiation balance of the atmosphere as well as the
34 activation of clouds and reduce the albedo of different cryospheric components like snow and glaciers enhancing
35 the melting of snow and ice after deposition. Arctic aerosols exhibit a pronounced seasonal cycle with high
36 concentrations in winter and early spring and lower values in summer (Law and Stohl, 2007; Quinn et al., 2007;
37 Eleftheriadis et al., 2009). This seasonality is caused by different processes related to emission, transport, and
38 deposition, which undergo seasonal cycles (Law and Stohl, 2007; Croft et al., 2016).



39 Sea spray, dust, and biogenic aerosol particles are important natural aerosol types in the Arctic. In contrast,
40 Arctic BC stems primarily from regions outside the Arctic (Law and Stohl, 2007). Like in all marine
41 environments, sea salt aerosol (SSA) dominates the atmospheric aerosol burden over the Arctic Ocean and its
42 coastal areas (e.g. Geng et al., 2010; Weinbruch et al., 2012). The production and climatic effects of SSA in the
43 Arctic are expected to change in the future as a result of changes in the sea ice cover and ocean temperatures
44 (Struthers et al., 2011; Zábory et al., 2013). Dust may act as effective ice nuclei in the Arctic (Si et al., 2018) and
45 may have the potential to influence radiative and other properties of mixed-phase cold clouds.

46 The removal due to deposition controls the lifetime of aerosols and in the Arctic determines the input of the
47 aerosols to the snow and glaciers. In fact, the past atmospheric input has been reconstructed from ice cores in the
48 Arctic (Legrand and Mayewski, 1997; Isaksson et al., 2003; Bauer et al. 2013). Moreover, the deposition of BC
49 to cryospheric components like snow and sea ice also impacts the local and regional climate in the Arctic due to
50 the lowering of the snow albedo and associated albedo feedback processes (e.g. Flanner et al., 2007; Bond et al.,
51 2013; Jacobi et al., 2015). The removal results from wet deposition caused by precipitation and dry deposition of
52 particles, which depend on aerosols size, meteorological conditions, and properties of the atmospheric boundary
53 layer. Despite its importance the deposition of the aerosols to the cryosphere is not well quantified for many
54 polar sites and even the respective contributions of wet and dry deposition are not well known for many
55 compounds (Legrand and Mayewski, 1997; Bauer et al. 2013). As a result, the recommended method to
56 determine dry deposition relies mostly on the calculation of fluxes based on atmospheric composition and an
57 estimated dry deposition velocity (Vet et al., 2014), which shows, however, a large uncertainty. In the case of
58 BC, the calculated deposition varies considerably across models since it depends on the applied assumptions and
59 parameters concerning the size of the aerosols and the mixing state (Bond et al., 2013). For example, the
60 estimated total BC deposition in the Arctic varies between 8 and more than 13 Tg C yr⁻¹ with the dry deposition
61 contributing between a few and up to 40 % of the total removal (Liu et al., 2011). Although a comprehensive
62 understanding of microphysics and chemistry related to aging and deposition is essential for a successful
63 simulation of BC concentrations over the Arctic (Liu et al., 2011; Sharma et al., 2013), direct BC deposition
64 measurements are still limited. In addition, the few available measurements of average dry deposition of
65 submicron particles over snow also show a large range from 0.02 to 0.33 cm s⁻¹ (Duan et al., 1988; Contini et al.,
66 2010; Grönlund et al., 2002).

67 While detailed investigations of the chemical properties of aerosols have been performed at Ny-Ålesund based
68 on single particle analysis (e.g. Geng et al., 2010; Weinbruch et al., 2012) similar studies for the composition of
69 the precipitation and the snow pack are currently missing. Moreover, due to the rapid changes in aerosol sources
70 it is urgent to better quantify the fate of different aerosol types in the Arctic. Here, we combine observations in
71 the snow pack and the atmosphere to better constrain deposition processes for major and minor sea salt
72 components and BC around Ny-Ålesund, Svalbard during the winter period. We used meteorological
73 observations to perform detailed physical snow pack modeling. The results of such simulations are to our
74 knowledge for the first time combined with precipitation and atmospheric aerosol measurements to derive
75 chemical profiles and monthly snow budgets related to dry and wet deposition. The calculated profiles are finally
76 compared to physical and chemical snow pack measurements to evaluate the performance of the snow pack
77 model and to improve our understanding of the deposition processes. Variations in the concentrations of multiple

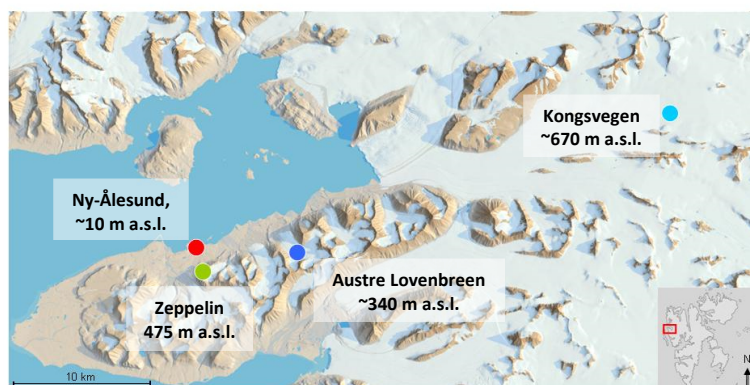


78 species in aerosols, precipitation, and in the snowpack are used to study the transfer processes from the
79 atmosphere to the snow for the investigated species.

80 2 Methods

81 2.1 Snow sampling

82 Sampling of snow was performed in snow pits on two glaciers located approximately 8 and 35 km to the east of
83 Ny-Ålesund, Svalbard (Fig. 1). The snow was sampled on 30 March 2012 on the Kongsvegen glacier (snow pit
84 KV, 78.755° N, 13.337° E, ~670 m a.s.l.) and on 13 April 2012 on the Austre Lovénbreen glacier (snow pit
85 AL, 78.871° N, 12.150° E, ~340 m a.s.l.). In both cases, pits were dug down to the ice layer formed during the
86 summer/fall period in 2011. The sampled snow pack, thus, represented the precipitation accumulated during the
87 previous winter period. For both snow pits the stratigraphy was established based on visual inspection of the
88 different layers following international guidelines (Fierz et al., 2009). Snow density was measured using a 250
89 cm³ triangular snow cutter. Furthermore, duplicate snow samples were collected using 50 mL polypropylene
90 tubes for either chemical or BC analysis. The tubes with an inner diameter of 2.7 cm were horizontally inserted
91 into the wall of the snow pit after careful cleaning of the snow surface. The below reported depths of the snow
92 samples correspond to the center of the tube openings. Furthermore, three fresh snow samples were collected
93 within 12 h after the end of the precipitation on 24 (two samples) and 29 March at a distance of ~5 km from the
94 village of Ny-Ålesund, which were analyzed for BC.



95
96 **Fig. 1:** 3D map of the Kongsfjord area with Ny-Ålesund (red), Zeppelin Station (green) and the locations of the snow
97 pits on the Kongsvegen (light blue) and the Austre Lovénbreen glaciers (dark blue) indicated (©Norwegian Polar
98 Institute).

99 2.2 Snow analysis

100 All samples were stored at -20°C at Ny-Ålesund, transported frozen to Grenoble using isolated boxes and stored
101 further at -20°C until analysis. Concentrations of the components sodium, potassium, magnesium, calcium,
102 chloride, sulfate, nitrate, and bromide were determined using ion chromatography in one of the duplicate snow
103 samples. The samples were filtered using 0.22 µm Acrodisc filters before analysis. Anions and cations were
104 analyzed with a combined suppressed conductivity Dionex ICS3000 instrument using AS11-HC and CS12
105 columns. The detection limit is typically below 1 ppb for all measured compounds. The analytical precision is
106 around 5 % for all ions. Five analyzed samples showed bromide concentrations below the detection limit (3



107 samples snow pit KV, 2 samples snow pit AL), which were replaced by values of 0.5 ppb for all further
108 calculations. Non sea salt-sulfate concentrations were calculated according to $[\text{nss-sulfate}] = [\text{sulfate}] - 0.2516 \cdot$
109 $[\text{sodium}]$ (Millero et al., 2008).

110 Refractory BC (rBC) was determined with a Single Particle Soot Photometer (SP2, Droplet Measurement
111 Technologies, USA). Details of the analytical procedure are described in Lim et al. (2014). Briefly, the SP2
112 allows quantifying the mass of single particles using a laser-induced incandescence technique. The instrument
113 has unity detection efficiency for rBC particles with diameters between 80 and 600 nm, while avoiding
114 interferences with other inorganic or organic species. The instrument was calibrated using size-selected fullerene
115 soot (Alfa Aesar Inc., USA). A commercial nebulizer (APEX-Q, Elemental Scientific Inc., Omaha, USA) was
116 used to transfer the particles from the melted snow to the aerosol phase. The losses during aerosolization were
117 determined daily using suspensions of Aquadag standards with different mass concentrations resulting in an
118 average efficiency of 56 %, which was applied to all reported rBC concentrations. Two samples from snow pit
119 AL showed rBC concentrations below the limit of quantification of 0.03 ppb (Lim et al., 2014), which was used
120 instead for all further calculations.

121 **2.3 Meteorological data**

122 Meteorological parameters have been recorded close to the analyzed snow pit KV by an energy balance station
123 (KNG8, Kärner et al., 2013). The station provided data on air temperature, wind speed, wind direction, short-
124 and longwave radiation components, and relative humidity. Surface height changes were recorded with an
125 ultrasonic ranger and allowed deriving accumulation (precipitation). If the measured surface raised more than 1
126 cm within one hour, the precipitation amount was calculated using a temperature- and wind speed-dependent
127 parameterization for the density of fresh snow also used in the Crocus model (Vionnet et al., 2012). As a result a
128 good agreement between observed and simulated increases in snow height was obtained. Cloud cover was
129 estimated from the ratio between observed and theoretical incoming shortwave radiation using the method
130 described in Jacobi et al. (2015).

131 **2.4 Snow pack modeling and snow budgets**

132 Simulations for the snow pack on the Kongsvegen glacier were performed with the one-dimensional multi-layer
133 physical snow pack model Crocus (Vionnet et al., 2012; Jacobi et al., 2010a; 2015), which was previously
134 applied for mass-balance simulations of the glacier (Sauter and Oblitner, 2015). The model solves the surface
135 mass and energy budgets taking into account physical processes like heat diffusion, transfer of radiation,
136 densification, sublimation, condensation, and melting. The model is forced using meteorological data like air
137 temperature, wind speed, relative humidity, precipitation rate and phase, incoming direct and diffuse short-wave
138 radiation, incoming long-wave radiation, and cloud cover. The forcing data for the period September 2011 to
139 March 2012 were generated from observations at the energy balance station KNG8. The model was initiated
140 with an ice layer set to a temperature of 0°C. The output refers to multiple homogeneous horizontal layers that
141 are established according to snowfall events and undergo transformation related to a metamorphism scheme. The
142 model delivers physical properties of each snow layer including thickness, density, temperature, structure
143 parameters and date of accumulation. According to the simulations the oldest conserved snow pack layer was
144 deposited on 30 October 2011. The simulations deliver accumulation dates for each simulated layer, which were



145 used to divide total snow budgets into monthly budgets for October 2011 and March 2012. However, the
146 incomplete October budgets were not used for further analysis. Concentrations and densities of the simulated
147 snow layers were used to calculate monthly budgets for each impurity.

148 2.5 Atmospheric concentrations

149 Atmospheric concentrations C_{atm} of ionic species in the aerosols were measured at Zeppelin Station at an altitude
150 of 475 m a.s.l.. The aerosols were collected using a three stage filterpack sampler with no size cut off (Aas et al.,
151 2013). The data were downloaded from the EBAS database (ebas.nilu.no) for the period from 30 October 2011
152 to 29 March 2012 as daily averages. Concentrations of atmospheric BC corresponding to equivalent BC (eBC)
153 were determined at the Zeppelin station using the 880 nm channel BC values recorded by a 7-wavelengths AE31
154 aethalometer (Eleftheriadis et al., 2009) using updated parameters for the absorption and attenuation according to
155 Backman et al. (2017) and Zanatta et al. (2018). Daily averages were used for further calculations (see
156 Supplementary Material, Fig. S1). The eBC time series includes 23 missing values (7 days in November, 16 days
157 in December) and 19 values below the detection limit (BDL) of 7 ng m^{-3} in the analyzed period. While the
158 missing values were replaced by the monthly averages, the impact of using either the maximum or minimum
159 value (7 or 0 ng m^{-3}) to replace the values BDL remained small for calculated monthly averages ($< 0.8 \text{ ng m}^{-3}$
160 and $< 7\%$). Therefore, all values BDL were replaced by 3.5 ng m^{-3} equal to half of the detection limit before
161 further calculations.

162 2.6 Dry and wet deposition

163 Dry deposition of particles (D_{dry} ; g m^{-2}) was calculated using Eq. (1),

$$164 D_{\text{dry}} = C_{\text{atm}} \cdot v_d \cdot t \cdot 10^{-6} \quad (1)$$

165 with the deposition velocity v_d in m s^{-1} , the atmospheric concentration of the aerosols C_{atm} in $\mu\text{g m}^{-3}$, and the
166 averaging time t for the atmospheric measurements (here 24 h). While wind speed- and particle size-dependent
167 parameterizations for v_d are available (e.g. Zhang et al., 2001), the use of single values of v_d to estimate dry
168 deposition fluxes from aerosol concentrations is still standard. Here, we used a high v_d value of 1 cm s^{-1} for the
169 ionic species assuming that they were mainly associated with coarse sea salt aerosols (Zhang et al., 2001). Thus,
170 we consider the estimated dry deposition of these components as an upper limit. The gas-phase species nitric
171 acid (HNO_3) and sulfur dioxide (SO_2) also contribute to the total dry deposition of nitrogen and sulfur, but are
172 not included in the estimates here. Since bromide was not determined in the aerosols, the standard sea water ratio
173 and observed sodium concentrations were used to estimate the dry deposition of bromide. A smaller v_d of 0.1 cm
174 s^{-1} was used for BC, which corresponds to a typical global annual mean in many models (Wang et al., 2011) and
175 is within the range of observed deposition velocities of sub-micron particles over snow (Duan et al., 1988;
176 Contini et al., 2010; Grönlund et al., 2002). The total and monthly dry deposition was calculated as the sum of
177 the daily deposition either for the full period or for each month from November 2011 to March 2012.

178 Wet deposition (D_{wet} ; g m^{-2}) was calculated using observed precipitation amounts (P ; L m^{-2}) and chemical
179 concentrations (C_{precip} ; mg L^{-1}) of the precipitation collected at Ny-Ålesund close to sea level using Eq. (2):

$$180 D_{\text{wet}} = C_{\text{precip}} \cdot P \cdot 0.001 \quad (2)$$

181 Major sea salt components and nitrate were determined using ion chromatography in precipitation samples
182 collected on a weekly basis using a bucket funnel system in summer and a snow sampler in winter (Kühnel et al.,



183 2011; Aas et al., 2013). The data downloaded from the EBAS database (ebas.nilu.no) were used without further
184 correction, although the bulk sampler likely collected also gaseous compounds and particulate material due to
185 dry deposition. Especially in periods with high wind speed, the bulk collector may also catch large sea spray
186 aerosols. However, the exact contribution of dry deposition to the here calculated wet deposition is difficult to
187 quantify since it depends on the frequency of rain events and episodes with elevated sea salt aerosols. The total
188 and monthly wet deposition was calculated as the sum for the period from 31 October 2011 to 1 April 2012 and
189 for each month (except October). No measurements of bromide and BC in the precipitation are available. For
190 bromide, wet deposition was estimated from the wet deposition of sodium applying the standard sea water
191 composition according to $D_{wet}(\text{bromide}) = 0.00624 \cdot D_{wet}(\text{sodium})$ (Millero et al., 2008). Wet deposition of BC
192 was estimated according to the scavenging scheme proposed by Sharma et al. (2013). The change in atmospheric
193 BC concentration $\Delta[BC]$ was estimated using the BC concentration $[BC]$, the scavenging coefficient (R ; $\text{m}^2 \text{kg}^{-1}$
194 $^{-1}$), the precipitation rate (P_t , $\text{L m}^{-2} \text{s}^{-1}$) and the time step (Δt , s) according to Eq. (3):

$$195 \Delta[BC] = [BC] \cdot R \cdot P_t \cdot \Delta t \quad (3)$$

196 We used a scavenging coefficient of $R = 5 \cdot 10^{-3} \text{ m}^2 \text{ kg}^{-1}$ as recommended by Sharma et al. (2013). Since all
197 scavenged atmospheric BC will be mixed into the accumulated weekly snowfall ($(P_t \cdot \Delta t)$), the BC concentration
198 in the snow $[BC]_{\text{snow}}$ in ppb is calculated according to Eq. (4), where h denotes the depth of the atmospheric
199 column affected by scavenging:

$$200 [BC]_{\text{snow}} = 10^{-9} \cdot [BC] \cdot h \cdot R \quad (4)$$

201 Since typical top heights of clouds in the wintertime Arctic are on the order of 4500 m (Intrieri et al., 2002) we
202 used $h = 4500$ m for the tropospheric column concerned by scavenging. BC concentrations in snow were
203 calculated only for weeks with precipitation recorded at Ny-Ålesund and using the observed weekly precipitation
204 rates. For further calculations, we used monthly average BC concentrations in the snow due to scavenging to
205 derive monthly wet deposition according to Eq. (2). Finally, total wet deposition corresponds here to the sum of
206 the monthly wet deposition from November to March.

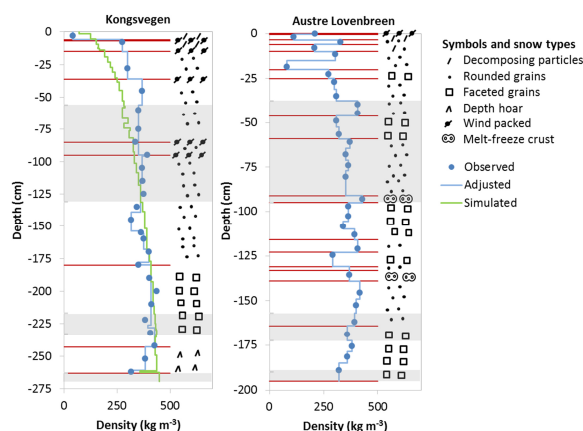
207 **3 Results and discussion**

208 **3.1 Physical properties of the snow pack**

209 The stratigraphy and densities for the two analyzed snow pits are shown in Fig. 2. The investigated snow layers
210 comprised depths down to -263 cm below the surface for snow pit KV and -195 cm for snow pit AL reaching in
211 both cases the surface of the ice layer formed during the previous summer. While both snow pits showed a
212 typical increase in density from the surface to the deeper layers, the variability in terms of grain types and layer
213 structures was higher for snow pit AL. At an altitude of 670 m a.s.l. the high wind speeds at snow pit KV led to
214 the formation of several wind-packed layers. The impact of significant melting was not identified in the snow pit
215 KV, although the recorded temperatures reached several times values above or close to the melting point (see
216 Supplementary Material, Fig. S2). In contrast, at an altitude of 340 m a.s.l. melting events were more apparent in
217 snow pit AL, which exhibited several melt freeze crusts probably due to warmer periods in November 2011 and
218 January 2012 accompanied by air temperatures above 0°C and large amounts of rain at sea level in Ny-Ålesund.
219 The stronger impact of melting in the snow pit AL was confirmed by the chemical composition. The ratio of
220 magnesium to sodium has been proposed as a melt indicator (Iizuka et al., 2002; Virkkunen et al., 2007; Ginot et



221 al., 2010) with lower ratios caused by the preferential removal of magnesium due to percolating water. While the
222 average magnesium to sodium ratios were around 0.12 in both snow pits, in snow pit AL the variability was
223 higher and minimum values lower. Smallest ratios were encountered in layers deposited in November, January,
224 and March corresponding to the months with elevated air temperatures. Nevertheless, in both snow pits the ratios
225 did not reach the small ratios as observed in ice cores from Svalbard (Iizuka et al., 2002; Virkkunen et al., 2007).
226 Therefore, a certain redistribution of the impurities probably occurred in the snow pack due to melting, but not a
227 complete removal. While the impact was stronger on the Austre Lovenbreen glacier, the overall budgets of both
228 snow pits seemed not to be influenced.
229



230

231 **Fig. 2: Snow stratigraphy observed in the snow pits KV (left) and AL (right). Note the different depth scales. Snow**
232 **types are indicated on the right side using the classification recommended by Fierz et al. (2009) with layers separated**
233 **by horizontal red lines. Blue circles indicate observed snow densities, vertical blue lines correspond to snow densities**
234 **adjusted to observed and sampled layers. The green line shows snow densities simulated with the Crocus model for**
235 **snow pit KV. The alternating shaded and non-shaded areas correspond from the top to the months March to October.**

236 Together with the stratigraphy, full snow density profiles were established for both pits as shown in Fig. 2.
237 According to these profiles, the total accumulation amounts to 943 and 667 mm snow water equivalent (SWE)
238 for the snow pits KV and AL. The accumulation in the pit KV was close to the maximum observed in the years
239 2007 to 2009 at altitudes above 600 m on the Kongsvegen glacier (Forsström et al., 2013). The observed
240 accumulation of precipitation at Ny-Ålesund close to sea level corresponds to a value of 278 mm for the period
241 from 31 October 2011 to 01 April 2012. The gradient in accumulation between the snow pits KV, AL, and Ny-
242 Ålesund was slightly higher than 30 % per 100 m altitude increase and is, thus, close to accumulation gradients
243 previously applied for the nearby Midre Lovénbreen and Austre Brøggerbreen glaciers (Hodson et al., 2005).
244 Crocus model results obtained for the snow pit KV were used here for further analysis. The snow pack simulated
245 for 29 March 2012 consists of 50 layers with varying densities covering a total depth of -269.4 cm (Fig. 2). The
246 densities below -80 cm are well represented by the model, but the densities between -10 and -80 cm are
247 underestimated compared to the observations. While density measurements using a cutter suffer from a
248 systematic overestimation (Proksch et al., 2016), a strong bias in simulated snow densities in the top layers is
249 common for snow models applied to polar regions (e.g. Groot Zwaafink et al., 2013). Despite the differences in
250 the top layers, the simulated total SWE of 937 mm is in excellent agreement with the observed SWE. Shaded
251 areas in Fig. 2 indicate the different layers deposited in the months from October 2011 to March 2012 according



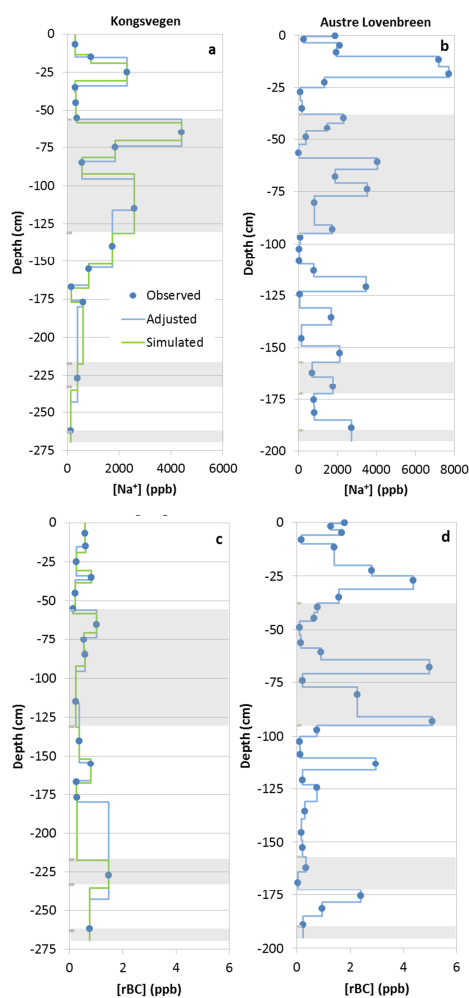
252 to the simulations. Only complete identified snow layers were attributed to specific months. Assuming a constant
253 linear decrease in accumulation from the snow pit KV to AL, monthly layers were also attributed to snow pit AL
254 with linearly interpolated depth ranges using the ratio of the total snow heights of both pits (Fig. 2).

255 3.2 Impurity profiles in the snow pack

256 Co-located impurity profiles were established for each measured compound combining the measured
257 concentrations with either the observed stratigraphy for both snow pits or the simulated stratigraphy for snow pit
258 KV. Figure 3 shows as examples the observed sodium and rBC concentrations as well as the profiles. Some
259 common features can be identified for sodium in the upper part of both snow pits. Snow pit KV showed three
260 layers with elevated concentrations: a first peak in the March layer around -25 cm, and a double peak in the
261 February layer with a maximum around -60 cm and a broad maximum below -100 cm (Fig. 3a). A comparable
262 pattern was found in snow pit AL with the strongest peak in the March layer at -20 cm and two maxima in
263 February at -40 cm and a broad peak between -60 and -90 cm (Fig. 3b). However, the relative strengths of the
264 peaks are different in the two pits. While these differences may be caused by site-dependent deposition fluxes,
265 they may also be related to melt-water formation and percolation, which likely had a stronger impact on snow pit
266 AL. This may have contributed also to the higher variability of sodium in the lower part of the snow pit AL
267 compared to KV. Moreover, peaks may have been missed at KV because of the larger spacing between the
268 samples.

269 The lowest concentrations of all studied impurities were found for rBC. Average rBC concentrations differed by
270 a factor of two between the two location with 0.6 ppb at KV (Fig. 3c) and 1.2 ppb at AL (Fig. 3d). The average
271 concentration at AL is in good agreement with the average rBC concentration of (1.4 ± 0.2) ppb for the snow
272 pack accumulated during the winter 2012/2013 on the Brøggerbreen glacier at 300 m altitude (Sinha et al.,
273 2018). However, the concentrations are lower than elemental carbon (EC) measured with a thermo-optical
274 method in samples from the Kongsvegen glacier above 600 m a.s.l., where Forsström et al. (2013) found median
275 concentrations of 1.4, 4.2, and 3.8 ppb in April 2007, 2008, and 2009. It should be noted here and during all
276 further discussion, that the comparison of the different quantities EC, eBC, and rBC introduces additional
277 uncertainties. For example, a previous comparison of EC and rBC in snow samples from Greenland indicated a
278 mean ratio of two (Lim et al., 2014), while atmospheric rBC and eBC measurements in Ny-Ålesund are more
279 consistent if adjusted absorption properties are used (Zanatta et al., 2018). These uncertainties may partly explain
280 the differences in the determined concentrations. While an overall decrease of atmospheric BC concentrations in
281 the Arctic (Sinha et al., 2017) potentially contributed to lower concentrations in 2012 compared to the years
282 2007 to 2009, the impact is difficult to analyze due to large inter-annual meteorological variabilities impacting
283 the transport of BC to the Arctic (Eleftheriadis et al., 2009; Hirdmann et al., 2010) occasionally leading to high
284 pollution events in wintertime (e.g. Winiger et al., 2012). Melting processes probably caused the higher
285 variability of BC in the AL pit since insoluble particles show enrichments at the snow surface generating layers
286 with enhanced concentrations in the Arctic (Forsström et al., 2013).

287



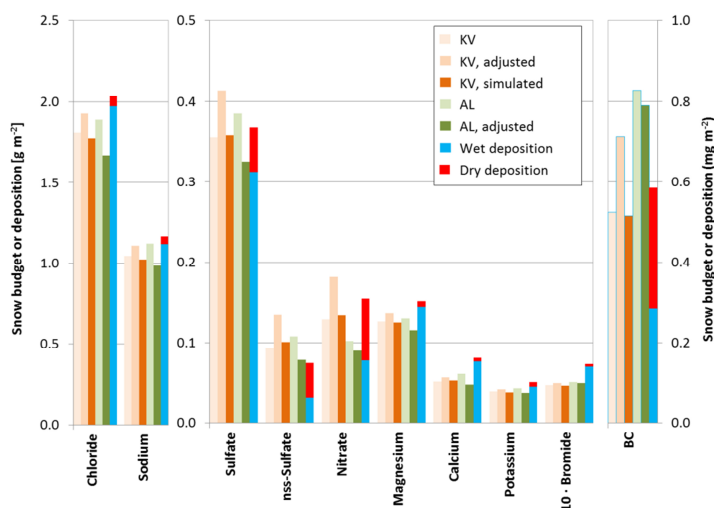
288

289
290
291
292
293

Fig. 3: Sodium (top) and rBC concentrations (bottom) in the snow pits KV (left) and AL (right). Blue circles indicate observed concentrations and blue lines correspond to concentrations adjusted to the observed stratigraphy. The green line shows concentrations adjusted to the simulated stratigraphy for the snow pit KV. The alternating shaded and non-shaded areas correspond from the top to the months March to October.

294 3.3 Wintertime snow budgets and deposition of ionic compounds

295 Total snow budgets of all measured compounds for the two snow pits were calculated using three different
296 approaches: (i) simple budgets were determined by multiplying the average concentrations by the total SWE; (ii)
297 adjusted budgets were calculated from the interpolated density profile shown in Fig. 2 and co-located
298 concentration profiles like in Fig. 3; (iii) for snow pit KV simulated budgets were obtained by combining the
299 simulated density profiles with simulated concentration profiles. All calculated budgets are summarized in Fig.
300 4, which also shows the observed wet deposition at Ny-Ålesund and the estimated total dry aerosol deposition
301 for the period from 31 October 2011 to 29 March 2012. According to the meteorological records of the
302 Norwegian Meteorological Service (eklima.met.no) no further precipitation occurred between 29 March and 15
303 April 2012 and the total wet deposition can, thus, be compared to the budget of the snow pit AL.



304
 305 **Fig. 4:** Snow budgets of sea salt components, nss-sulfate, nitrate and bromide (left and middle) and BC (right) for the
 306 snow pits KV (Kongsvegen, brown) and AL (Austre Lovénbreen, green) for October 2011 to March 2012 according to
 307 different calculation methods: simple budgets from average concentrations and total SWE (light colors), adjusted
 308 budgets using co-located concentration and density profiles (middle colors), and simulated budgets for KV using
 309 interpolated concentration and simulated density profiles (dark colors). Also shown is the total deposition as the sum
 310 of observed wet deposition at Ny-Ålesund (blue) and estimated dry particle deposition (red). For bromide the wet
 311 deposition was estimated from the standard sea water ratio and all numbers are multiplied by ten. For BC the snow
 312 budgets correspond to rBC, while the wet deposition was estimated for the KV snow pit. The BC deposition
 313 corresponds to eBC. See text for further details.

314 Due to errors of the manual snow density measurements, the chemical analysis, and the extrapolation of the
 315 density and concentration profiles, it can be assumed that differences in the budgets below 20 % as obtained for
 316 chloride, sodium, magnesium, calcium, and potassium are not significant. The spatial variability of snow
 317 concentrations at a scale of meters can be even larger (e.g. Svensson et al., 2013). Thus, the total snow budgets
 318 for the pits KV and AL reveal a consistent picture for the sea salt components chloride, sodium, magnesium,
 319 potassium, and bromide (Fig. 4). For these species neither the method for the calculation of the total budgets, the
 320 location, the altitude, nor the accumulation led to significant differences in the observed total budgets. This is
 321 consistent with recent observations revealing characteristic patterns of aerosol concentrations along Svalbard
 322 glaciers including the Kongsvegen demonstrating consistent formation, transport, and exchange processes
 323 between the atmosphere and the snow (Spolaor et al., 2017).

324 If post-depositional processes are negligible, the total snow budgets of the impurities correspond to the input due
 325 to the sum of the wet and dry deposition. Based on the comparison of the total snow budgets with the observed
 326 wet deposition, the estimated dry deposition are evaluated for the different impurities. The total snow budgets of
 327 chloride, sodium, magnesium, and potassium agree well with the observed wet deposition at Ny-Ålesund with
 328 differences smaller than 20 % for the period from October 2011 to March/April 2012. However, the recorded
 329 wet deposition also includes variable contributions from dry deposition since the precipitation samples were
 330 collected with an open bucket instrument (Kühnel et al., 2011). Nevertheless, the estimated dry deposition
 331 corresponds to less than 5 % of the wet deposition of chloride, sodium, and magnesium and reaches a maximum
 332 of 14 % for potassium (Fig. 4). Subtracting the nss-sulfate from the total sulfate shows that the dry deposition of
 333 sulfate with marine origin also corresponds to less than 5 % of the total wet deposition. Since the estimated dry
 334 deposition is considered as an upper limit, it can be assumed that its contribution for the total snow budget on the



335 Kongsvegen and Austre Lovenbreen glaciers during the period November 2011 to April 2012 remained small for
336 chloride, sodium, magnesium, potassium, and sea salt sulfate. The estimated wet deposition for bromide based
337 on sodium concentrations and the standard sea water ratio leads to an overestimation of more than 40 %
338 compared to the observed bromide in the snow pack (Fig. 4). This demonstrates that sea salt bromide is
339 undergoing important modifications during the formation of sea salt aerosols, in the atmosphere, or after
340 deposition (see Sect. 3.7).

341 Like for the sea salt components, a good agreement between the KV snow budget of nitrate and nss-sulfate and
342 the total deposition during the period from October 2011 to April 2012 is found. For these two compounds the
343 observed wet deposition at Ny-Ålesund remains significantly below the snow budget, while the missing fractions
344 are largely compensated by the estimated dry deposition. For nitrate, the dry deposition is comparable to the wet
345 deposition, whereas for nss-sulfate dry deposition even dominates the snow budget. The adjusted budgets of the
346 snow pit AL show ~50 % less nitrate and ~40 % less nss-sulfate compared to KV (Fig. 4), which may be related
347 to the spatial variability of the dry deposition of the two species.

348 **3.4 Wintertime snow budgets and deposition of BC**

349 Regarding the snow budgets, the different average rBC concentrations are partly compensated by the different
350 accumulation for the two snow pits. The simple, adjusted, and simulated snow budgets vary between 0.51 and
351 0.71 mg m⁻² for KV and 0.79 and 0.83 mg m⁻² for AL and are, thus, between 10 and 60 % higher at AL
352 compared to KV. Albeit the difference between EC and rBC (see Sect. 3.2), it appears that the derived rBC
353 budget for KV remain well below the EC budgets for 2007 to 2009 for the Kongsvegen glacier (Forsström et al.,
354 2013). In contrast, the AL budget is somewhat above the rBC budget for the Brøggerbreen glacier of 0.49 mg m⁻²
355 determined in April 2013 (Sinha et al., 2018). These differences probably also correspond to the inter-annual
356 variability of BC as reflected in the atmospheric observations (Eleftheriadis et al., 2009).

357 The BC deposition derived here only relies on estimated values for scavenging and dry deposition velocities.
358 Nevertheless, the monthly averages of the estimated BC concentrations in fresh snow due to scavenging varying
359 from 0.2 ppb in October 0.8 ppb in March. The March average is in very good agreement with the three fresh
360 snow samples collected in March 2012, which showed rBC concentrations of 0.47, 0.72, and 0.97 ppb,
361 respectively. Moreover, these estimated concentrations are in agreement with average eBC concentrations in
362 fresh snow samples collected in April and November in the years 2012 to 2017 on the glaciers surrounding Ny-
363 Ålesund ranging from 0.9 to 2 ppb (Gogoi et al., 2018). Finally, Noone and Clarke (1988) proposed a
364 dimensionless scavenging ratio (SR) corresponding to the quotient of the atmospheric and snow concentration of
365 BC. Using the observed atmospheric BC and the estimated BC concentrations in snow we derive SRs of
366 approximately 30, which agree with the lower end of SRs for the Ny-Ålesund area (Gogoi et al., 2016; 2018).

367 The anti-correlation between accumulation and the average BC concentrations in the two snow pits points to an
368 important contribution of dry deposition, which is in agreement with the estimated dry and wet deposition of BC.
369 The dry deposition of eBC (Fig. 4) derived with a deposition velocity of 0.1 cm s⁻¹ corresponds to approximately
370 half of the observed rBC budget at KV and is, thus, somewhat higher than the contribution due to wet deposition.
371 Despite the overall uncertainty related to the simplified methods for the estimation of the BC deposition, the
372 difference between the snow budgets and the total deposition remain below 25 % for the KV and below 45 % for
373 the AL snow pit. This important contribution of dry deposition is in contrast to wet and total deposition reported



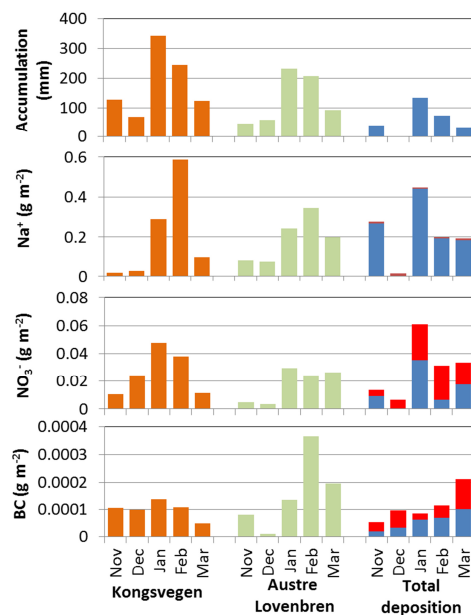
374 for Ny-Ålesund for the winter 2012/2013 based on rBC measurements in falling snow and in the snow pack
375 (Sinha et al., 2018). From these observations it was concluded that the dry deposition of rBC remained
376 negligible. However, the authors also reported rBC fluxes at 300 m altitude on the Broggerbreen glacier, which
377 were twice as high as in Ny-Ålesund. While Sinha et al. (2018) claim that this increase is mainly due to the
378 higher accumulation on the glacier, additional dry deposition at higher altitudes cannot be excluded. Moreover,
379 the potential contamination of the snow pack close to Ny-Ålesund due to local power generation or a potential
380 mismatch between the budgets of the falling snow and the snow pack due to the removal by blowing snow were
381 not considered.

382 Previous model studies have indicated that BC in the Arctic is primarily removed through wet deposition (e.g.
383 Flanner et al., 2007; Wang et al., 2011). However, in the models the dry deposition velocity of BC was often
384 reduced to improve the simulated atmospheric concentrations of BC. Moreover, the here observed wintertime
385 deposition may not be extrapolated to the entire Arctic since the BC deposition depends on multiple factors like
386 air mass transport, aging processes of atmospheric BC particles, and ice nucleation (e.g. Sharma et al., 2013; Liu
387 et al., 2011; Vergara-Temprado et al., 2018)

388 3.5 Comparison of monthly snow budgets and deposition

389 To derive a higher temporal resolution of the snow budgets monthly snow budgets were calculated from layers
390 deposited in each month between November 2011 and March 2012. The monthly budgets are further compared
391 to monthly wet and dry deposition. Each weekly wet deposition was attributed to the month with the largest
392 overlap in time to derive the monthly wet deposition, while the monthly dry deposition was calculated from the
393 daily dry deposition. Monthly total deposition was calculated as the sum of the corresponding wet and dry
394 deposition. Figure 5 shows as example the results for sodium, nitrate, and BC. Results similar to sodium were in
395 general obtained for the other sea salt components. The dominating role of wet deposition for sodium and other
396 sea salt components and the larger contribution of dry deposition for nitrate and BC are also reflected in the
397 monthly budgets. For the months with recorded precipitation at Ny-Ålesund, the wet deposition of sea salt
398 components largely dominates the total deposition. This is in contrast to nitrate and BC, which show several
399 monthly budgets with higher values for dry than wet deposition.

400 The generally good agreement between the total budgets of the two snow pits and the wet and dry deposition
401 (Fig. 4) is only partly confirmed by the monthly budgets shown in Fig. 5. For example, the monthly budgets of
402 sodium show a much more pronounced variability at KV compared to AL. In contrast, the monthly total
403 deposition shows a very low value for December due to the lack of wet deposition observed at Ny-Ålesund and
404 no clear cycle for the remaining months. Similar results are obtained for other sea-salt components. In general,
405 differences are caused by multiple reasons related to uncertainties in the forcing data, in the model results as well
406 as in the spatial variability of the observations in the snow, wet deposition, and aerosol concentrations.
407 Moreover, post-depositional processes modifying the derived monthly snow budgets like blowing snow or
408 melting processes are currently not taken into account in the simulations. Nevertheless, it appears that for
409 compounds with a larger contribution of dry deposition the agreement between snow budgets and total
410 deposition is somewhat better like in the cases of nitrate and BC (Fig. 5).



411
412
413
414
415
416

Fig. 5: Monthly accumulation and snow budgets for sodium, nitrate, and BC for the snow pits KV (Kongsvegen, orange) and AL (Austre Lovénbreen, green) according to the simulated profiles. Also shown is the observed accumulation at Ny-Alesund (top, blue) and the total deposition divided into wet (blue) and dry (red) deposition. For sodium and nitrate the wet deposition was measured at Ny-Ålesund and the wet deposition for BC was estimated from scavenging. The BC snow budgets correspond to rBC, while the wet and dry depositions correspond to eBC.

417

3.6 Variations of the chemical composition of snow, aerosols, and precipitation

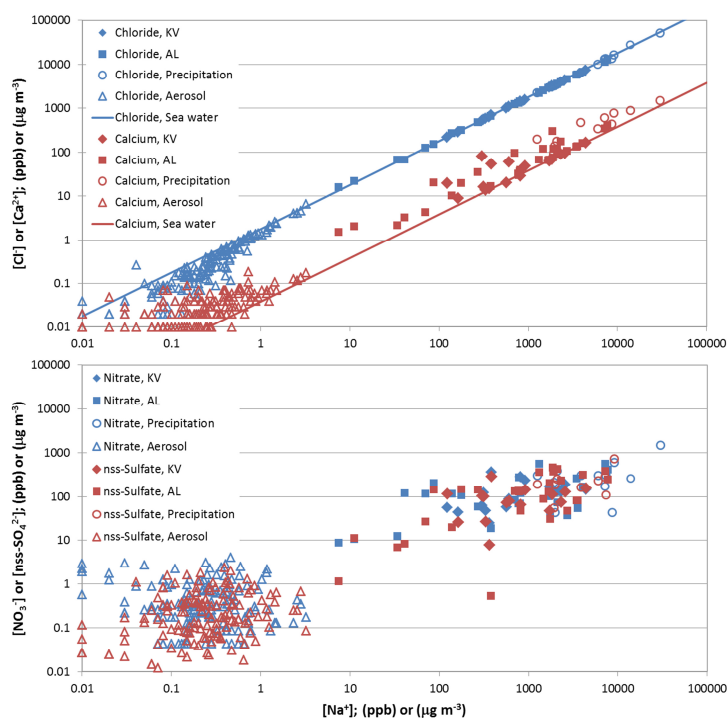
418

Variation diagrams showing the concentrations of two trace compounds are often exploited to determine common sources or processes acting upon the correlated species. Here, the ratios of concentrations in the atmosphere, the precipitation, and the snow are used to study the transfer processes from the atmosphere to the snow. Figure 6 shows the variation of chloride vs sodium for the period from October 2011 to April 2012 in aerosols at Zeppelin Station, in the precipitation at Ny-Ålesund, and in the snow pits KV and AL. Most of the chloride-to-sodium ratios in the aerosols are close to the standard sea water ratio (Millero et al., 2008) indicating that in the marine environment around Ny-Ålesund the composition of the aerosols is dominated by sea salt. Some aerosol samples show dechlorination likely caused by the replacement of chlorine ions due to the uptake of sulfuric and nitric acid (Keene et al., 1998). Figure 6 demonstrates further that the impact of the dechlorination becomes visible only during periods with low atmospheric loading of sea salt aerosols with less than $1 \mu\text{g m}^{-3}$ sodium. Such a dechlorination, however, is masked in the precipitation and snow samples, which were all close to the standard sea water ratio. In summary, in wintertime the composition of the majority of the aerosols as well as the precipitation around Ny-Ålesund is dominated by sea salt aerosols confirming previous studies of individual aerosol particles (Weinbruch et al., 2012). This leads to the same chemical imprint in the snow pack. Magnesium and potassium show a similar variation with sodium (not shown), except that some aerosol samples showed elevated potassium concentrations possibly due to potassium-enriched dust particles from soils. Nevertheless, the variation in the precipitation samples confirms that the contribution of dry aerosol deposition remained small also for these compounds with respect to the overall observed budget of the snow pits.

436



437



438

439

440

441

442

Fig. 6, upper panel: Chloride (blue) and calcium (red) concentrations vs. sodium concentrations in snow pit KV (filled diamonds) and AL (filled squares), in precipitation (open circles) and in aerosols (open triangles). Aerosol concentrations are in $\mu\text{g m}^{-3}$ and are derived from measurements at Zeppelin Station. The lines indicate the standard sea water ratio. **Lower panel:** Same as top, but for nitrate (blue) and nss-sulfate (red).

443

Calcium shows a different behavior compared to the other major sea salt components with a significant enrichment of calcium in the aerosols as well as in the precipitation, which also causes calcium-to-sodium ratios above standard sea water in a large number of snow samples (Fig. 6). Such an enrichment in the Arctic may be attributed to calcium-rich aerosols originating from soils (Toom-Sauntry and Barrie, 2002; Geng et al., 2010; Jacobi et al., 2012; Weinbruch et al., 2012) although local aerosol formation was probably limited due to the extended snow cover. The in- or below-cloud scavenging of dust particles likely contributed to the transfer of the elevated calcium concentrations from the aerosols to the precipitation and to the snow.

450

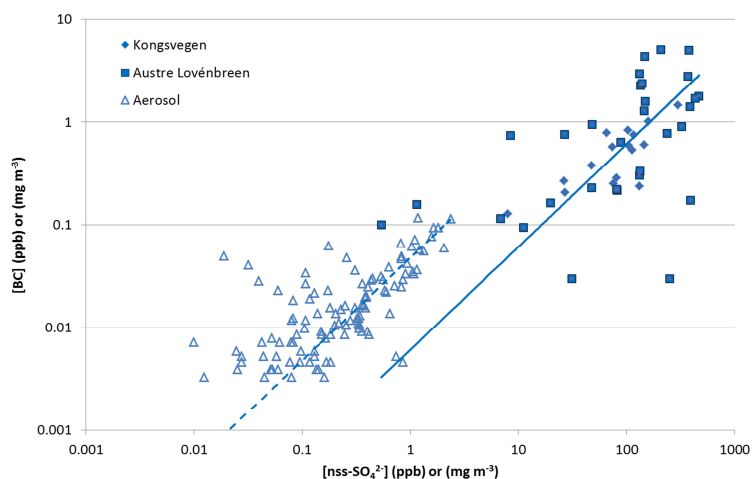
Like demonstrated in previous studies (e.g. Jacobi et al., 2012), nitrate and nss-sulfate in aerosols, in the precipitation, and in the snow do not exhibit a constant ratio compared to sodium (Fig. 6). On average, highest and lowest ratios are found in the aerosols and in the precipitation with the average snow pack ratio in between these values. This confirms that the nitrate and nss-sulfate in the snowpack can be attributed to a mixture of wet deposition and dry deposition of aerosols. Although in wintertime the reactive nitrogen budget is dominated by particulate nitrate (Hara et al., 1999), a further dry deposition of gas phase species to the snow is possible, which may be even more important than the aerosol deposition (Björkman et al., 2013).

457

Due to the different sources of BC and sodium (long-range transport vs local or regional formation of sea salt aerosols), no consistent BC-to-sodium variation is found in the aerosols (Supplementary material, Fig. S3). Similarly, the variation of BC in the snow pits is also independent of the sodium concentrations. Since BC particles are preferentially coated by organic matter or sulfate (Liu et al., 2011), atmospheric BC shows a linear



461 relationship to nss-sulfate resulting in a correlation coefficient R^2 of 0.60 (Fig. 7). In the snowpack, the rBC-to-
462 nss-sulfate ratios are less consistent and the average ratio is almost one order of magnitude smaller than in the
463 atmosphere. Despite the different measurement techniques for BC in the aerosols and in the snow, the lower BC-
464 to-nss-sulfate ratio in the snow can only partly be explained by the different measurement methods. Different
465 ratios in the snow may be caused by the smaller contribution of wet to total deposition of BC as compared to nss-
466 sulfate (Fig. 4). Moreover, the AL snow pit shows a higher variability in the BC-to-nss-sulfate variation than the
467 KV snow pit (Fig. 7) indicating that redistribution of the impurities caused by melting probably also impacted
468 BC and nss-sulfate.



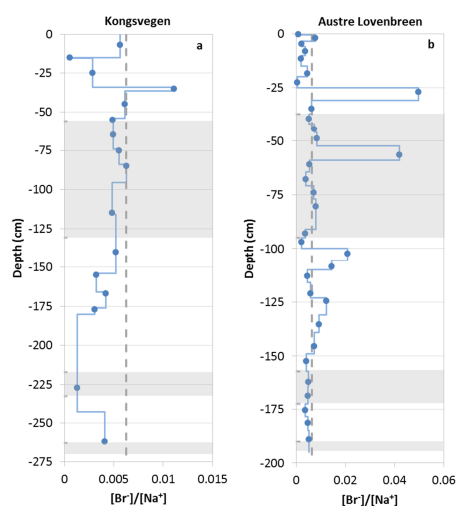
469 Fig. 7: BC vs. nss-sulfate concentrations in snow pit KV (filled diamonds) and AL (filled squares), and in aerosols
470 (open triangles). The lines calculated by linear regression are forced through the origin and separated for the aerosol
471 and the snow samples. BC in the snow pits corresponds to rBC, while the BC in aerosols corresponds to eBC.
472

473 3.7 Bromide in the snowpack

474 Since no bromide concentrations in the aerosols and in the precipitation are available, the ratio between bromide
475 and sodium is shown in the form of profiles for the snow pits KV and AL (Fig. 8). The ratio between the overall
476 bromide and sodium budgets varies between 0.0045 for KV and 0.005 for AL and is, thus, below the standard
477 sea water ratio of 0.00624 (Millero et al., 2008). Only distinct layers show enrichments of bromide (Fig. 8).
478 Multiple photochemical processes occur in the sea ice-snow-atmosphere system of the Arctic acting upon the
479 variation between bromide and sodium (Simpson et al., 2007; Jacobi et al., 2012). On solid surfaces (aerosols,
480 snow, sea ice) bromide can be transformed into volatile bromine compounds that are released to the atmosphere
481 and are subsequently deposited. Therefore, bromide can be depleted already in the sea salt aerosols generated
482 over sea ice, which would cause a wet and dry deposition flux lower than estimated based on the standard sea
483 water ration, or it can be diminished in the surface snow after deposition (Jacobi et al., 2012) explaining the
484 average bromide-to-sodium ratios below the sea water ratio in both snow pits. Nevertheless, since the released
485 bromide is subsequently deposited, a snow pack with layers enriched in bromide is also possible depending on
486 the dominating influence of the release vs the additional deposition of bromide (Simpson et al., 2007). This can
487 also explain the contrasting results found on top of the Holtedahlfonna glacier, located approximately 40 km to
488 the Northeast of Ny-Ålesund in April 2012. Spolaor et al. (2013) reported that the snow pack was highly
489 enriched in bromide with only a few samples close to the sea water ratio potentially caused by the additional



490 deposition of bromide after release from sea ice-covered areas of the Arctic Ocean. It is well known that such
491 activation of bromide mainly occurs in springtime after polar sunrise explaining the low bromide budgets in the
492 KV and AL snow pits in the winter period. Since the bromine activation over sea ice also leads to a significant
493 destruction of tropospheric ozone (Jacobi et al., 2010b), the ozone record at Zeppelin Station may be used as a
494 proxy for the impact of bromine-rich air masses at Ny-Ålesund and the surrounding area. The ozone
495 concentration during the entire period covered by the snow pits remained above 35 ppbV and dropped to ~20
496 ppbV on the afternoon of 29 March (data accessible at ebas.nilu.no) indicating that the influence of bromine-
497 enriched air remained small in spring 2012 before the sampling of the snow pits. Finally, meteorological
498 conditions in Ny-Ålesund are less sensitive to the sea ice extent than other locations in Svalbard according to a
499 study of precipitation trends (Osuch and Wawrzyniak, 2016). Thus, the distinct peaks in the bromide-to-sodium
500 in the snow pit AL, which occurred in layers attributed to early March, late-February, and late January are
501 probably not caused by additional deposition as a consequence of bromine explosion events, but are possibly
502 related to the influence of melting. Accordingly, these high ratios are not produced by enhanced bromide, but by
503 low sodium concentrations. In summary, the potential use of bromide enrichment as proxy for the bromine
504 activation and, thus, sea ice extent as developed by Spolaor et al. (2013) for the Holtedahlfonna record appears
505 rather limited for the snow pack and glaciers around Ny-Ålesund due to a restricted impact of sea ice conditions
506 in this region.
507



508 **Fig. 8: Bromide-to-sodium ratio in the snow pits KV (left) and AL (right). Blue circles indicate observed ratios; blue**
509 **lines correspond to ratios adjusted to the observed stratigraphy. The alternating non-shaded areas correspond to the**
510 **months November, December, January, February, and March (from the bottom). The vertical dashed grey lines**
511 **indicate the standard sea water ratio.**
512

513 4 Conclusion

514 The chemical composition of aerosols, precipitation, and the snow pack was analyzed for Ny-Alesund, Svalbard.
515 The results concerning the snow budgets, the wet deposition, and the ratios of the different components in the
516 snow pack, in the precipitation, and in the aerosols underline the importance of wet deposition for the major sea-



517 salt components chloride, sodium, potassium, magnesium, and sulfate during the winter period from October
518 2011 to March 2012 confirming previous studies (Isaksson et al., 2003; Weinbruch et al., 2012; Geng et al.,
519 2010). The significant contribution of wet deposition is further supported by the estimated upper limit of the dry
520 aerosol deposition. Although the choice of the deposition velocity introduces considerable uncertainty, the
521 estimated dry deposition remains well below 10 % of the total deposition for chloride, sodium, and magnesium,
522 while it contributes more than 20 % to the snow budget of calcium and potassium probably due to a stronger dust
523 contribution. It is possible that the relatively high overall accumulation including strong precipitation events in
524 the last week of January contributed to the high input due to wet deposition during the winter 2011/2012.
525 Therefore, the contribution of dry deposition of sea salt aerosols could be larger during winter periods with
526 different precipitation characteristics. Nevertheless, it appears that the wet deposition measurements at Ny-
527 Ålesund can be used to estimate the total wintertime deposition of the major sea salt components in the areas
528 surrounding Ny-Ålesund.

529 In contrast to the major sea salt components the dry deposition of nitrate and nss-sulfate was more important
530 than the wet deposition. However, the dry deposition of the corresponding gas phase species like HNO_3 and SO_2
531 are not well quantified (e.g. Zhang et al., 2001; Osada et al., 2010) and probably contributed also to the observed
532 snow budgets of nitrate and sulfate. Further direct measurements of the dry deposition of all N-containing
533 species and nss-sulfate would be needed to better quantify the full N- and S-cycle in the Arctic.

534 The obtained results for the snow budgets and the deposition of BC indicate a behavior of BC resembling nitrate
535 and nss-sulfate. In the wintertime the deposition of BC to the snowpack on the glaciers surrounding Ny-Ålesund
536 appears to be equally driven by dry and wet deposition. However, it is important to note the large uncertainties in
537 the estimated BC deposition, for which direct measurements in the Arctic are needed. Overall, the average rBC
538 concentrations in the wintertime snowpack remained below 1.2 ppb and, thus, causing a marginal reduction of
539 the snow albedo. In contrast, post-depositional processes are likely at the origin of snow layers with rBC
540 concentrations increased by a factor of three compared to the average. Such layers may cause a stronger direct
541 and indirect impact on the snow albedo via enhanced metamorphism processes (e.g. Jacobi et al., 2015). Further
542 studies with detailed observations of the vertical BC distribution in the snow pack are required for a better
543 quantification of the climate impact of BC in snow.

544 Bromide is the sea salt compound showing the strongest variability in the ratio to other major components like
545 sodium, which is related to its high mobility in the sea ice-atmosphere-snow system caused by chemical
546 processes. Systematic measurements of bromide not only in the snowpack, but also in the aerosols, in the
547 precipitation, and in fresh snow are required to further investigate processes before the formation of the sea salt
548 aerosols, during their transport, or after the deposition to the snow pack.

549 While the annual budgets and estimated deposition for most of the studied species agree well, the results for the
550 monthly budgets obtained with the detailed snowpack modeling are less convincing. Further improvements
551 regarding the modeling of the Arctic snow pack are needed to better address physical properties (e.g. the
552 evolution of the snow density) and post-depositional processes acting upon the vertical distribution of impurities
553 in the snow pack. Although the treatment of impurities was recently implemented into the Crocus snowpack
554 model (Tuzet et al., 2017), the impact of processes modifying the vertical distribution of impurities in the Arctic
555 snowpack like blowing snow, sublimation, and percolation are still not fully considered in most models. The full



556 implementation of post-depositional processes into complex snow models may offer the opportunity to exploit
557 further snow pack and ice core observations for the reconstruction of climate and pollution.

558

559 *Code and data availability.* The snowpack scheme Crocus is integrated into the surface modeling platform
560 SURFEX developed by Météo-France. The SURFEX code is freely available via www.umr-cnrm.fr/surfex/
561 using a CECILL-C license. The snow pit (<https://doi.org/10.6096/parcs.12>, <https://doi.org/10.6096/parcs.13>) and
562 the meteorological data (<https://doi.org/10.6096/parcs.17>) are available from the PARCS data base ([www4.obs-](http://www4.obs-mip.fr/parcs/database/)
563 [mip.fr/parcs/database/](http://www4.obs-mip.fr/parcs/database/)). Precipitation data are available from the EBAS data base of the Norwegian Institute for
564 Air Research (ebas.nilu.no). BC data is available on request.

565

566 *Author contributions.* HWJ performed the snow sampling, the simulations, and the analysis and wrote the
567 manuscript. FO provided meteorological data for the simulations, advice during the analysis, and support in
568 writing the manuscript. SDC contributed to the snow sampling and analysis. PG performed the chemical analysis
569 of the snow samples. KE provided atmospheric BC data. WA provided precipitation data. PG, KE, and WA
570 contributed to the writing of the manuscript. MZ contributed to the snow sampling, performed the BC analysis of
571 the snow samples, and provided support in writing and designing the manuscript.

572

573 *Competing interests.* The authors declare that they have no conflict of interest.

574

575 *Acknowledgments.* The research project No. 1030 (CLIMSLIP-NyA) was performed at the AWIPEV Station. It
576 was supported by the French Polar Institute (IPEV), the Agence Nationale de la Recherche under the contract
577 ANR 2011 Blanc SIMI 5-6 021 04, by Campus France (No. 31597SM) and the Austrian Science Fund (FWF,
578 grant I 369-B17), by the Chantier Arctique Francais (CNRS/INSU) via the project PARCS, and by the Labex
579 OSUG@2020 (Investissements d'avenir – ANR10 LABX56). MZ gratefully acknowledges the funding by the
580 Deutsche Forschungsgemeinschaft (DFG, German Research Foundation) – Projektnummer 268020496 – TRR
581 172, within the Transregional Collaborative Research Center “Arctic Amplification: Climate Relevant
582 Atmospheric and SurfaCe Processes, and Feedback Mechanisms (AC)³. The KV weather station is operated in
583 cooperation with the Norwegian Polar Institute (Tromsø). The measurements of major inorganic ions in
584 precipitation and aerosols at Ny Ålesund and Zeppelin are part of the national atmospheric monitoring financed
585 by the Norwegian Environment Agency.

586 References

587 Aas, W., Solberg, S., Manø, S., and Yttri, K. E.: Monitoring of long-range transported air pollutants. Annual
588 report for 2012 (In Norwegian), NILU Norwegian Institute for Air Research, Kjeller, NILU Scientific Reports
589 OR 14/2013, 216 pp., 2013.

590 Backman, J., Schmeisser, L., Virkkula, A., Ogren, J. A., Asmi, E., Starkweather, S., Sharma, S., Eleftheriadis,
591 K., Uttal, T., Jefferson, A., Bergin, M., Makshtas, A., Tunved, P., and Fiebig, M.: On Aethalometer
592 measurement uncertainties and an instrument correction factor for the Arctic, Atmos. Meas. Tech., 10, 5039-
593 5062, <https://doi.org/10.5194/amt-10-5039-2017>, 2017.



- 594 Bauer, S. E., Bausch, A., Nazarenko, L., Tsigaridis, K., Xu, B., Edwards, R. Bisiaux, M., and McConnell, J.:
595 Historical and future black carbon deposition on the three ice caps: Ice core measurements and model
596 simulations from 1850 to 2100, *J. Geophys. Res. Atmos.*, 118, 7948–7961, <https://doi.org/10.1002/jgrd.50612>,
597 2013.
- 598 Björkman, M. P., Kühnel, R., Partridge, D. G., Roberts, T. J., Aas, W., Mazzola, M., Viola, A., Hodson, A.,
599 Ström, J., and Isaksson, E.: Nitrate dry deposition in Svalbard, *Tellus B*, 65,
600 <https://doi.org/10.3402/tellusb.v65i0.19071>, 2013.
- 601 Bond, T. C., Doherty, S. J., Fahey, D.W., Forster, P. M., Berntsen, T., De Angelo, B. J., Flanner, M. G., Ghan,
602 S., Kärcher, B., Koch, D., Kinne, S., Kondo, Y., Quinn, P. K., Sarofim, M. C., Schultz, M. G., Schulz, M.,
603 Venkataraman, C., Zhang, H., Zhang, S., Bellouin, N., Guttikunda, S. K., Hopke, P. K., Jacobson, M. Z., Kaiser,
604 J. W., Klimont, Z., Lohmann, U., Schwarz, J. P., Shindell, D., Storelvmo, T., Warren, S. G., and Zender, C. S.:
605 Bounding the role of black carbon in the climate system: A scientific assessment, *J. Geophys. Res. Atmos.*, 118,
606 5380–5552, <https://doi.org/10.1002/jgrd.50171>, 2013.
- 607 Contini, D., Donato, A., Belosi, F., Grasso, F. M., Santachiara, G., and Prodi, F.: Deposition velocity of
608 ultrafine particles measured with the Eddy-Correlation Method over the Nansen Ice Sheet (Antarctica), *J.*
609 *Geophys. Res.*, 115, D16202, <https://doi.org/10.1029/2009JD013600>, 2010.
- 610 Croft, B., Martin, R. V., Leaitch, W. R., Tunved, P., Breider, T. J., D'Andrea, S. D., and Pierce, J. R.: Processes
611 controlling the annual cycle of Arctic aerosol number and size distributions, *Atmos. Chem. Phys.*, 16, 3665-
612 3682, <https://doi.org/10.5194/acp-16-3665-2016>, 2016.
- 613 Duan, B., Fairall, C. W., and Thomson, D. W.: Eddy Correlation measurements of the dry deposition of particles
614 in wintertime, *J. Appl. Meteor.*, 27, 642–652, [https://doi.org/10.1175/1520-0450\(1988\)027<0642:ECMOTD>2.0.CO;2](https://doi.org/10.1175/1520-0450(1988)027<0642:ECMOTD>2.0.CO;2), 1988.
- 616 Eleftheriadis, K., Vratolis, S., and Nyeki, S.: Aerosol black carbon in the European Arctic: Measurements at
617 Zeppelin station, Ny-Ålesund, Svalbard from 1998–2007, *Geophys. Res. Lett.*, 36, L02809,
618 <https://doi.org/10.1029/2008GL035741>, 2009.
- 619 Fierz C., Armstrong R. L., Durand Y., Etchevers P., Greene E., McClung D. M., Nishimura K., Satyawali P. K.,
620 and Sokratov, S. A.: The international classification for seasonal snow on the ground, UNESCO-IHP, Paris, IHP-
621 VII Technical Documents in Hydrology No. 83, IACS Contribution No. 1, 80 pp., 2009.
- 622 Flanner, M. G., Zender, C. S., Randerson, J. T., and Rasch, P. J.: Present-day climate forcing and response from
623 black carbon in snow, *J. Geophys. Res.*, 112, D11202, <https://doi.org/10.1029/2006JD008003>, 2007.
- 624 Forsström, S., Isaksson, E., Skeie, R. B., Ström, J., Pedersen, C. A., Hudson, S. R., Berntsen, T. K., Lihavainen,
625 H., Godtliebsen, F., and Gerland, S.: Elemental carbon measurements in European Arctic snow packs, *J.*
626 *Geophys. Res. Atmos.*, 118, 13,614–13,627, <https://doi.org/10.1002/2013JD019886>, 2013.
- 627 Geng, H., Ryu, J. Y., Jung, H.-J., Chung, H., Ahn, K.-H., and Ro, C.-U.: Single-particle characterization of
628 summertime arctic aerosols collected at Ny-Alesund, Svalbard, *Environ. Sci. Technol.*, 44, 2348-2353,
629 <https://doi.org/10.1021/es903268j>, 2010.
- 630 Ginot, P., Schotterer, U., Stichler, W., Godoi, M. A., Francou, B., and Schwikowski, M.: Influence of the
631 Tungurahua eruption on the ice core records of Chimborazo, Ecuador, *The Cryosphere*, 4, 561-568,
632 <https://doi.org/10.5194/tc-4-561-2010>, 2010.



- 633 Gogoi, M.M., Babu, S. S., Moorthy, K. K., Thakur, R. C., Chaubey, J. P., and Nair, V. S.: Aerosol black carbon
634 over Svalbard regions of Arctic, *Polar Sci.*, 10, 60-70, <https://doi.org/10.1016/j.polar.2015.11.001>, 2016.
- 635 Gogoi, M.M., Babu, S. S., Pandey, S. K., Nair, V. S., Vaishya, A., Girach, I. A., and Koushik, N.: Scavenging
636 ratio of black carbon in the Arctic and the Antarctic, *Polar Sci.*, 16, 10-22,
637 <https://doi.org/10.1016/j.polar.2018.03.002>, 2018.
- 638 Grönlund, A., Nilsson, D., Koponen, I., Virkkula, A., and Hansson, M.: Aerosol dry deposition measured with
639 eddy-covariance technique at Wasa and Aboa, DronningMaud Land, Antarctica. *Ann. Glaciol.*, 35, 355-361.
640 <https://doi.org/10.3189/172756402781816519>, 2002.
- 641 Groot Zwaartink, C. D., Cagnati, A., Crepez, A., Fierz, C., Macelloni, G., Valt, M., and Lehning, M.: Event-
642 driven deposition of snow on the Antarctic Plateau: analyzing field measurements with SNOWPACK, *The*
643 *Cryosphere*, 7, 333-347, <https://doi.org/10.5194/tc-7-333-2013>, 2013.
- 644 Hara, K., Osada, K., Hayashi, M., Matsunaga, K., Shibata, T., Iwasaka, Y., and Furuya, K.: Fractionation of
645 inorganic nitrates in winter Arctic troposphere: Coarse aerosol particles containing inorganic nitrates, *J.*
646 *Geophys. Res.*, 104 (D19), 23671–23679, <https://doi.org/10.1029/1999JD900348>, 1999.
- 647 Hirdman, D., Burkhart, J. F., Sodemann, H., Eckhardt, S., Jefferson, A., Quinn, P. K., Sharma, S., Ström, J., and
648 Stohl, A.: Long-term trends of black carbon and sulphate aerosol in the Arctic: changes in atmospheric transport
649 and source region emissions, *Atmos. Chem. Phys.*, 10, 9351-9368, <https://doi.org/10.5194/acp-10-9351-2010>,
650 2010.
- 651 Hodson, A. J., Mumford, P. N., Kohler, J., and Wynn, P. M.: The High Arctic glacial ecosystem: New insights
652 from nutrient budgets, *Biogeochem.*, 72, 233-256, <https://doi.org/10.1007/s10533-004-0362-0>, 2005.
- 653 Intrieri, J. M., Shupe, M. D., Uttal, T., and McCarty, B. J.: An annual cycle of Arctic cloud characteristics
654 observed by radar and lidar at SHEBA, *J. Geophys. Res.*, 107 (C10), <https://doi.org/10.1029/2000JC000423>,
655 2002.
- 656 Iizuka, Y., Igarashi, M., Kamiyama, K., Motoyama, H., and Watanabe, O.: Ratios of Mg² /Na in snowpack and
657 an ice core at Austfonna ice cap, Svalbard, as an indicator of seasonal melting, *J. Glaciol.*, 48 (162), 452-460.
658 <https://doi.org/10.3189/172756502781831304>, 2002.
- 659 Isaksson, E., Hermanson, M., Hicks, S., Igarashi, M., Kamiyama, K., Moore, J., Motoyama, H., Muir, D.,
660 Pohjola, V., Vaikmäe, R., van de Wal, R. S. W., and Watanabe, O.: Ice cores from Svalbard-useful archives of
661 past climate and pollution history, *Phys. Chem. Earth*, 28, 1217-1228, <https://doi.org/10.1016/j.pce.2003.08.053>,
662 2003.
- 663 Jacobi, H.-W., Domine, F., Simpson, W. R., Douglas, T. A., and Sturm, M.: Simulation of the specific surface
664 area of snow using a one-dimensional physical snowpack model: implementation and evaluation for subarctic
665 snow in Alaska, *The Cryosphere*, 4, 35-51, <https://doi.org/10.5194/tc-4-35-2010>, 2010a.
- 666 Jacobi, H.-W., Morin, S., and Bottenheim, J. W.: Observation of widespread depletion of ozone in the springtime
667 boundary layer of the central Arctic linked to mesoscale synoptic conditions, *J. Geophys. Res.*, 115, D17302,
668 <https://doi.org/10.1029/2010JD013940>, 2010b.
- 669 Jacobi, H. W., Voisin, D., Jaffrezo, J. L., Cozic, J., and Douglas, T. A.: Chemical composition of the snowpack
670 during the OASIS spring campaign 2009 at Barrow, Alaska, *J. Geophys. Res.*, 117, D00R13,
671 <https://doi.org/10.1029/2011JD016654>, 2012.



- 672 Jacobi, H.-W., Lim, S., Ménégoz, M., Ginot, P., Laj, P., Bonasoni, P., Stocchi, P., Marinoni, A., and Arnaud, Y.:
673 Black carbon in snow in the upper Himalayan Khumbu Valley, Nepal: observations and modeling of the impact
674 on snow albedo, melting, and radiative forcing, *The Cryosphere*, 9, 1685-1699, [https://doi.org/10.5194/tc-9-](https://doi.org/10.5194/tc-9-1685-2015)
675 1685-2015, 2015.
- 676 Karner, F., Obleitner, F., Krismer, T., Kohler, J., and Greuell, W.: A decade of energy and mass balance
677 investigations on the glacier Kongsvegen, Svalbard, *J. Geophys. Res. Atmos.*, 118, 3986–4000,
678 <https://doi.org/10.1029/2012JD018342>, 2013.
- 679 Keene, W.C., Sander, R., Pszenny, A. A. P., Vogt, R., Crutzen, P. J., and Galloway, J. N.: Aerosol pH in the
680 marine boundary layer: A review and model evaluation, *J. Aerosol Sci.*, 29, 339-356,
681 [https://doi.org/10.1016/S0021-8502\(97\)10011-8](https://doi.org/10.1016/S0021-8502(97)10011-8), 1998.
- 682 Kühnel, R., Roberts, T. J., Björkman, M. P., Isaksson, E., Aas, W., Holmén, K., and Ström, J.: 20-year
683 climatology of NO_3^- and NH_4^+ wet deposition at Ny-Alesund, Svalbard, *Adv. Meteorol.*, 406508,
684 <https://doi.org/10.1155/2011/406508>, 2011.
- 685 Law, K. S. and Stohl, A.: Arctic air pollution: Origins and impacts, *Science*, 315, 1537-1540,
686 <https://doi.org/10.1126/science.1137695>, 2007.
- 687 Legrand, M. and Mayewski, P.: Glaciochemistry of polar ice cores: A review, *Rev. Geophys.*, 35 (3), 219–243,
688 <https://doi.org/10.1029/96RG03527>, 1997.
- 689 Lim, S., Faïn, X., Zanutta, M., Cozic, J., Jaffrezo, J.-L., Ginot, P., and Laj, P.: Refractory black carbon mass
690 concentrations in snow and ice: method evaluation and inter-comparison with elemental carbon measurement,
691 *Atmos. Meas. Tech.*, 7, 3307-3324, <https://doi.org/10.5194/amt-7-3307-2014>, 2014.
- 692 Liu, J., Fan, S., Horowitz, L. W., and Levy II, H.: Evaluation of factors controlling long-range transport of black
693 carbon to the Arctic, *J. Geophys. Res.*, 116, D04307, <https://doi.org/10.1029/2010JD015145>, 2011.
- 694 Millero, F. J., Feistel, R., Wright, D. G. and McDougall, T. J.: The composition of Standard Seawater and the
695 definition of the Reference-Composition Salinity Scale, *Deep-Sea Res. I*, 55, 50-72,
696 <https://doi.org/10.1016/j.dsr.2007.10.001>, 2008.
- 697 Noone, K. J. and Clarke, A. D.: Soot scavenging measurements in arctic snowfall, *Atmos. Environ.*, 22, 2773-
698 2778, [https://doi.org/10.1016/0004-6981\(88\)90444-1](https://doi.org/10.1016/0004-6981(88)90444-1), 1998.
- 699 Osada, K., Shido, Y., Iida, H., and Kido, M.: Deposition processes of ionic constituents to snow cover, *Atmos.*
700 *Environ.*, 44, 347-353, <https://doi.org/10.1016/j.atmosenv.2009.10.031>, 2010.
- 701 Osuch, M. and Wawrzyniak, T.: Inter- and intra-annual changes in air temperature and precipitation in western
702 Spitsbergen, *Int. J. Climatol.*, <https://doi.org/10.1002/joc.4901>, 2016.
- 703 Proksch, M., Rutter, N., Fierz, C., and Schneebeli, M.: Intercomparison of snow density measurements: bias,
704 precision, and vertical resolution, *The Cryosphere*, 10, 371-384, <https://doi.org/10.5194/tc-10-371-2016>, 2016.
- 705 Quinn, P. K., Shaw, G., Andrews, E., Dutton, E. G., Ruoho-Airola, T., and Gong, S. L.: Arctic haze: current
706 trends and knowledge gaps, *Tellus B*, 59 (1), 99-114, <https://doi.org/10.1111/j.1600-0889.2006.00236.x>, 2007.
- 707 Sauter, T. and Obleitner, F.: Assessing the uncertainty of glacier mass-balance simulations in the European
708 Arctic based on variance decomposition, *Geosci. Model Dev.*, 8, 3911-3928, [https://doi.org/10.5194/gmd-8-](https://doi.org/10.5194/gmd-8-3911-2015)
709 3911-2015, 2015.



- 710 Sharma S., Ishizawa, M., Chan, D., Lavoué, D., Andrews, E., Eleftheriadis, K., and Maksyutov, S.: 16-year
711 simulation of Arctic black carbon: Transport, source contribution, and sensitivity analysis on deposition, *J.*
712 *Geophys. Res. Atmos.*, 118, 943–964, <https://doi.org/10.1029/2012JD017774>, 2013.
- 713 Shindell, D.: Local and remote contributions to Arctic warming, *Geophys. Res. Lett.*, 34, L14704,
714 <https://doi.org/10.1029/2007GL030221>, 2007.
- 715 Simpson, W. R., von Glasow, R., Riedel, K., Anderson, P., Ariya, P., Bottenheim, J., Burrows, J., Carpenter, L.
716 J., Frieß, U., Goodsite, M. E., Heard, D., Hutterli, M., Jacobi, H.-W., Kaleschke, L., Neff, B., Plane, J., Platt, U.,
717 Richter, A., Roscoe, H., Sander, R., Shepson, P., Sodeau, J., Steffen, A., Wagner, T., and Wolff, E.: Halogens
718 and their role in polar boundary-layer ozone depletion, *Atmos. Chem. Phys.*, 7, 4375–4418,
719 <https://doi.org/10.5194/acp-7-4375-2007>, 2007.
- 720 Si, M., Irish, V. E., Mason, R. H., Vergara-Temprado, J., Hanna, S. J., Ladino, L. A., Yakobi-Hancock, J. D.,
721 Schiller, C. L., Wentzell, J. J. B., Abbatt, J. P. D., Carslaw, K. S., Murray, B. J., and Bertram, A. K.: Ice-
722 nucleating ability of aerosol particles and possible sources at three coastal marine sites, *Atmos. Chem. Phys.*, 18,
723 15669–15685, <https://doi.org/10.5194/acp-18-15669-2018>, 2018.
- 724 Sinha, P. R., Kondo, Y., Koike, M., Ogren, J. A. Jefferson, A., Barrett, T. E., Sheesley, R. J., Ohata, S., Moteki,
725 N., Coe, H., Liu, D., Irwin, M., Tunved, P., Quinn, P. K., and Zhao, Y.: Evaluation of ground-based black carbon
726 measurements by filter-based photometers at two Arctic sites, *J. Geophys. Res. Atmos.*, 122, 3544–3572,
727 <https://doi.org/10.1002/2016JD025843>, 2017.
- 728 Sinha, P. R., Kondo, Y., Goto-Azuma, K., Tsukagawa, Y., Fukuda, K., Koike, M., Ohata, S., Moteki, N., Mori,
729 T., Oshima, N., Förland, E. J., Irwin, M., Gallet, J.-C., and Pedersen, C. A.: Seasonal progression of the
730 deposition of black carbon by snowfall at Ny-Ålesund, Spitsbergen. *J. Geophys. Res. Atmos.*, 123, 997–1016.
731 <https://doi.org/10.1002/2017JD028027>, 2018.
- 732 Spolaor, A., Gabrieli, J., Martma, T., Kohler, J., Björkman, M. B., Isaksson, E., Varin, C., Vallenga, P., Plane,
733 J. M. C., and Barbante, C.: Sea ice dynamics influence halogen deposition to Svalbard, *The Cryosphere*, 7, 1645-
734 1658, <https://doi.org/10.5194/tc-7-1645-2013>, 2013.
- 735 Spolaor, A., Barbaro, E., Mazzola, M., Viola, A. P., Lisok, J., Obleitner, F., Markowicz, K. M., and Cappelletti,
736 D.: Determination of black carbon and nanoparticles along glaciers in the Spitsbergen (Svalbard) region
737 exploiting a mobile platform, *Atmos. Environ.*, 170, 184–196, <https://doi.org/10.1016/j.atmosenv.2017.09.042>,
738 2017.
- 739 Struthers, H., Ekman, A. M. L., Glantz, P., Iversen, T., Kirkevåg, A., Mårtensson, E. M., Seland, Ø., and
740 Nilsson, E. D.: The effect of sea ice loss on sea salt aerosol concentrations and the radiative balance in the
741 Arctic, *Atmos. Chem. Phys.*, 11, 3459–3477, <https://doi.org/10.5194/acp-11-3459-2011>, 2011.
- 742 Svensson, J., Ström, J., Hansson, M., Lihavainen, H. and Kerminen, V.-M.: Observed metre scale horizontal
743 variability of elemental carbon in surface snow, *Environ. Res. Lett.*, 8, 034012, <https://doi.org/10.1088/1748-9326/8/3/034012>, 2013.
- 745 Toom-Sauntry, D. and Barrie, L. A.: Chemical composition of snowfall in the high Arctic: 1990–1994, *Atmos.*
746 *Environ.*, 36, 2683–2693, [https://doi.org/10.1016/S1352-2310\(02\)00115-2](https://doi.org/10.1016/S1352-2310(02)00115-2), 2002.
- 747 Tuzet, F., Dumont, M., Lafaysse, M., Picard, G., Arnaud, L., Voisin, D., Lejeune, Y., Charrois, L., Nabat, P., and
748 Morin, S.: A multilayer physically based snowpack model simulating direct and indirect radiative impacts of



- 749 light-absorbing impurities in snow, *The Cryosphere*, 11, 2633-2653, <https://doi.org/10.5194/tc-11-2633-2017>,
750 2017.
- 751 Vergara-Temprado, J., Holden, M. A., Orton, T. R., O'Sullivan, D., Umo, N. S., Browse, J., Reddington, C.,
752 Baeza-Romero, M. T., Jones, J. M., Lea-Langton, A., Williams, A., Carslaw, K.S., and Murray, B. J.: Is black
753 carbon an unimportant ice-nucleating particle in mixed-phase clouds? *J. Geophys. Res. Atmos.*, 123, 4273–4283.
754 <https://doi.org/10.1002/2017JD027831>, 2018.
- 755 Vet, R., Artz, R. S., Carou, S., Shaw, M., Ro, C.-U., Aas, W., Baker, A., Bowersox, V. C., Dentener, F., Galy-
756 Lacaux, C., Hou, A., Pienaar, J. J., Gillett, R., Forti, M. C., Gromov, S., Hara, H., Khodzher, T., Mahowald, N.
757 M., Nickovic, S., Rao, P. S. P., and Reid, N. W.: A global assessment of precipitation chemistry and deposition
758 of sulfur, nitrogen, sea salt, base cations, organic acids, acidity and pH, and phosphorus, *Atmos. Environ.*, 93, 3-
759 100, <https://doi.org/10.1016/j.atmosenv.2013.10.060>, 2014.
- 760 Virkkunen, K., Moore, J. C., Isaksson, E., Pohjola, V., Perämäki, P., Grinsted, A., and Kekonen, T.: Warm
761 summers and ion concentrations in snow: Comparison of present day with Medieval Warm Epoch from snow
762 pits and an ice core from Lomonosovfonna, Svalbard, *J. Glaciol.*, 53, 623-634,
763 <https://doi.org/10.3189/002214307784409388>, 2007.
- 764 Vionnet, V., Brun, E., Morin, S., Boone, A., Faroux, S., Le Moigne, P., Martin, E., and Willemet, J.-M.: The
765 detailed snowpack scheme Crocus and its implementation in SURFEX v7.2, *Geosci. Model Dev.*, 5, 773-791,
766 <https://doi.org/10.5194/gmd-5-773-2012>, 2012.
- 767 Wang, Q., Jacob, D. J., Fisher, J. A., Mao, J., Leibensperger, E. M., Carouge, C. C., Le Sager, P., Kondo, Y.,
768 Jimenez, J. L., Cubison, M. J., and Doherty, S. J.: Sources of carbonaceous aerosols and deposited black carbon
769 in the Arctic in winter-spring: implications for radiative forcing, *Atmos. Chem. Phys.*, 11, 12453-12473,
770 <https://doi.org/10.5194/acp-11-12453-2011>, 2011.
- 771 Weinbruch, S., Wiesemann, D., Ebert, M., Schütze, K., Kallenborn, R., and Ström, J.: Chemical composition and
772 sources of aerosol particles at Zeppelin Mountain (Ny Ålesund, Svalbard): An electron microscopy study,
773 *Atmos. Environ.*, 49, 142-150, <https://doi.org/10.1016/j.atmosenv.2011.12.008>, 2012.
- 774 Winiger, P., Andersson, A., Yttri, K. E., Tunved, P., and Gustafsson, Ö.: Isotope-based source apportionment of
775 EC aerosol particles during winter high-pollution events at the Zeppelin Observatory, Svalbard, *Environ. Sci.*
776 *Technol.*, 49, 11959-1966, <https://doi.org/10.1021/acs.est.5b02644>, 2012.
- 777 Zábori, J., Krejci, R., Ström, J., Vaattovaara, P., Ekman, A. M. L., Salter, M. E., Mårtensson, E. M., and Nilsson,
778 E. D.: Comparison between summertime and wintertime Arctic Ocean primary marine aerosol properties,
779 *Atmos. Chem. Phys.*, 13, 4783-4799, <https://doi.org/10.5194/acp-13-4783-2013>, 2013.
- 780 Zanatta, M., Laj, P., Gysel, M., Baltensperger, U., Vratolis, S., Eleftheriadis, K., Kondo, Y., Dubuisson, P.,
781 Winiarek, V., Kazadzis, S., Tunved, P., and Jacobi, H.-W.: Effects of mixing state on optical and radiative
782 properties of black carbon in the European Arctic, *Atmos. Chem. Phys.*, 18, 14037-14057,
783 <https://doi.org/10.5194/acp-18-14037-2018>, 2018.
- 784 Zhang, L., Gong, S., Padro, J., and Barrie, L.: A size-segregated particle dry deposition scheme for an
785 atmospheric aerosol module, *Atmos. Environ.*, 35, 549-560, [https://doi.org/10.1016/S1352-2310\(00\)00326-5](https://doi.org/10.1016/S1352-2310(00)00326-5),
786 2001.